Fall 2007

Pattern recognition of brain fMRI images for various physiological states

Priyanka Bhatt
New Jersey Institute of Technology

ABSTRACT

PATTERN RECOGNITION OF BRAIN FMRI IMAGES
FOR VARIOUS PHYSIOLOGICAL STATES

by
Priyanka Bhatt

The development of fMRI (functional Magnetic Resonance Imaging) has led many researchers to localize brain functions using different stimuli. The use of pattern recognition techniques have made it possible to predict the stimuli being presented from the corresponding brain images and activation patterns. The primary objective of the present study was to use pattern recognition methods to develop a model using available fMRI images and then to use the model to identify the stimulus presented from a large number of unknown images. Two different experimental conditions were used involving both binary and multi-class classification. Bilateral finger tapping data which had two distinct states "Active" and "Rest" were used for binary classification. Binary classification was done using Learning Vector Quantization (LVQ) and Least Square Support Vector Machine (LS-SVM). Gas mixture data, which were obtained from rats while ventilated with different gas mixtures for rest and breath hold task, gave various physiological conditions. These multi-class data were also classified using LS-SVM technique. Feature selection was performed on every data to select out patterns made up of significant voxels using statistical techniques like correlation, paired t-test and ANOVA. The accuracies for binary classification were between 90% and 100% while the average accuracy for multi-categorical data was 70%.

PATTERN RECOGNITION OF BRAIN FMRI IMAGES
FOR VARIOUS PHYSIOLOGICAL STATES

by
Priyanka Bhatt

**A Thesis
Submitted to the Faculty of
New Jersey Institute of Technology
in Partial Fulfillment of the Requirements for the Degree of
Master of Science in Biomedical Engineering**

Department of Biomedical Engineering

January 2008

Blank Page

APPROVAL PAGE

**PATTERN RECOGNITION OF BRAIN FMRI IMAGES
FOR VARIOUS PHYSIOLOGICAL STATES**

Priyanka Bhatt

Dr. Tara Alvarez, Co-Advisor	Date
Associate Professor of Biomedical Engineering, NJIT	

Dr. Bharat Biswal, Co-Adviser	Date
Associate Professor of Radiology, UMDNJ	

Dr. Richard Foulds, Committee Member	Date
Associate Professor of Biomedical Engineering, NJIT	

BIOGRAPHICAL SKETCH

Author: Priyanka Bhatt

Degree: Master of Science

Date: January 2008

Undergraduate and Graduate Education:

- Master of Science in Biomedical Engineering,
  New Jersey Institute of Technology, Newark, NJ, 2008

- Bachelor of Engineering in Biomedical and Instrumentation Engineering,
  U. V. Patel College of Engineering, Mehsana, Gujarat, 2005

Major: Biomedical Engineering

Kindly dedicated to my loving and caring family and my dear friends

ACKNOWLEDGMENT

TABLE OF CONTENTS

TABLE OF CONTENTS

TABLE OF CONTENTS

LIST OF TABLES

LIST OF FIGURES

CHAPTER 1

INTRODUCTION

1.1 Overview

Functional Magnetic Resonance Imaging (fMRI) is a non-invasive method with high spatial and temporal resolution to study brain function. The invention of fMRI has motivated many research laboratories to measure, quantify, and interpret the brain responses and a number brain functions have been revealed. The Brain has distinct identified regions for different sensorimotor and cognitive activities like visualizing, hearing, memorizing etcetera. These localized brain regions have been studied by "activating" these regions by applying specific known stimulations and outcomes can be studied to determine normal brain function. Blood oxygenation level dependence (BOLD) is the most common mechanism currently being used to measure signal changes in fMRI during brain activation.

Most fMRI studies have thus far been used to detect and quantify change in signal intensity when a stimulus/task is presented. Eloquent regions of the brain that undergo changes corresponding to the task are then identified using a number of appropriate statistical techniques. This mode of methodology and analysis is most commonly used in fMRI and has opened a large number of research avenues to pursue systems level neuroscience in both healthy and patient populations. Thus, fMRI has enabled researchers to non-invasively map different regions of the brain corresponding to specific types of stimulus. For example, the visual cortex and its associated regions have been mapped non-invasively on an individual basis and variations have been shown between them.

Clinically, it is being used for a number of applications including presurgical planning, language localization as an alternative Wada test and retinotopy mapping of the visual cortex.

While, the majority of the fMRI experiments are used to detect localize and quantify changes in signal intensity corresponding to a stimulus, some researchers have become interested in the inverse problem i.e. predicting the stimulus type by analyzing one or more fMRI images. Pattern Recognition is a very useful and popular technique in this field of research. This technique is typically used to categorize the activation maps from each of the stimulus/task into a unique set of multi-voxel patterns each corresponding to a specific stimulus/task. The procedure of identifying the stimulus for the given fMRI brain images is often referred as *brain reading*.

Currently, there are a large number of methods available to categorize and cluster information into different classes according to their distinct characteristics. Neural networks and Support Vector Machines are examples of classification tools. These techniques typically need some datasets with prior knowledge about their categories. They create a model (relating the input and output data sets) and train it using these data sets to classify them as per labels assigned and then use it to determine the class of test data set. For pattern recognition of fMRI images, fMRI images with known stimuli i.e. their labels which will be used for training and the output will be the identified stimulus of an unknown image or a set of images.

For effective classification, feature extraction plays a very important role. It discards common features present in every image and it selects only those voxels of the image which show maximum variety of responses to various stimuli. This is typically

done by selecting an appropriate mask and using statistical techniques including correlation, t-test, ANOVA and GLM.

In the present study, different algorithms were implemented which can identify different physiological conditions of the brain using fMRI images. Two different experiments were performed. In the first, binary classification method was used. In the second, multi-class classification methods was used. For the first experiment, finger tapping data was used which had two distinct states, "Activation" and "Rest". In the second experiment, multi-class classification was done using data obtained from animal models (rats). The images were acquired under normal breathing and breath hold with five different gas mixtures.

1.2 Objective

The purpose of the present study was to use fMRI brain images in conjunction with pattern analysis to predict the input stimulus used. Pattern analysis methods were utilized to prepare a model which can discriminate different physiological conditions of brain using fMRI images and identify the category of the unknown image accordingly. The first experiment was binary classification to categorize the "Active" and "Rest" states of images for finger tapping data. The second experiment was performed on the multi-categorical images which were acquired from rats while ventilated with different mixtures of gases. Normal breathing and breath hold were two tasks which were performed for each gas mixture and which created different physiological states of the brain. Various feature selection techniques and classification tools were tested in order to obtain the highest possible accuracy values.

1.3 Background Research

Pattern recognition for fMRI images is useful to classify similar looking images according to distinct activation patterns created by different brain responses. The concept of pattern recognition using multiple voxels has recently been reviewed by Norman, Detre and Haxby [1]. They stated that individual voxels contained in the image might not respond significantly to a particular task but selected group of voxels together would create a distinct pattern for distinct mental state. The pattern analysis study was very much dependent on the spatial preciseness of the images and therefore, they limited the experiments within individual subjects. The multi-voxel pattern analysis was used to find how well the voxels of particular region respond distinctively for different cognitive tasks. They also discussed about four basic steps that are required for successful pattern analysis of fMRI images. The four basic steps included, feature selection, pattern assembly, training classifiers and testing of classifiers.

Cox and Savoy (2003) used pattern recognition algorithms by dividing a high-dimensional space into different regions for different labels [2]. They classified the fMRI patterns created in the visual cortex due to different stationary visual stimuli. These visual stimuli were the objects covering wide variety of living and non living entities. In their study, as much as 30% of the brain volume covered by the images was discarded. They found classification accuracy well above chance, even when experiments were separated by days or weeks.

In another seminal study, Kamitani and Tong (2005) performed classification of the fMRI patterns for the perception of different edge orientations [3]. They introduced the concept called "ensemble feature selectivity" to explain the neural codes for different

perceptions. The stimuli for their study were finely spaced thin lines which were rotated at eight different angles to generate eight different orientations. They hypothesized that every voxel of 3 cubic mm area of visual cortex presents the signal change for different orientations. While this signal change might have been blurred due to limitations of fMRI acquisition, still the information taken from all voxels together presented a distinct pattern for each orientation. They could then identify the patterns using linear classifiers. The final accuracy was well accepted with only a few cases of misclassification which happened to be at neighboring orientations. Even when they showed overlapping orientations and asked subjects to concentrate on one of them, they were able to predict the attended orientation.

A very challenging job of multi-subject pattern recognition was undertaken and successfully implemented by Wang, Hutchinson and Mitchell (2003) [4]. For stimulation, they presented pictures and sentences to thirteen subjects in one study and a mixture of ambiguous and unambiguous sentences to five subjects in the second study. They used two different methods to compare the brain images of different subjects which were ROI mapping (for both experiments) and Talairach coordinates (for second experiment only). Both methods had some advantages and disadvantages and showed no significant difference in accuracies for classification for the second study.

1.4 Outline

This thesis document is organized in the following way. The second chapter explains the fundamentals of magnetic resonance imaging, MRI instrument and concepts of functional MR imaging. Chapter 3 is about data analysis performed on fMRI brain images using

motion correction technique, histogram study and feature selection. The pattern recognition is explained in chapter 4 which includes different classification tools like neural networks and LS-SVM. Chapter 5 explains data acquisition and methodology for both experiments. Chapter 6 describes outcomes of data analysis techniques and pattern recognition. Chapter 7 discusses some important aspects of this study and the conclusion.

CHAPTER 2

FUNDAMENTALS OF MAGNETIC RESONANCE IMAGING

Magnetic Resonance Imaging (MRI) is a modern and popular medical imaging modality. It has certain advantages over other available imaging tools like x-ray and CT scan as it does not involve any radiation. It provides very high resolution and better soft tissue contrast [5]. Functional MRI (fMRI) is the advancement of MRI which not only provides the view of the brain anatomy but also tracks the neurophysiological changes occurring in different regions and because of this ability it has become researchers' favorite tool to study the brain responses to different stimulations. This chapter discusses the basic topics related to MRI and fMRI including Nuclear Magnetic Resonance (NMR) principle, MR imaging, MRI instrumentation, BOLD contrast in fMRI, experimental design and fMRI artifacts.

2.1 Physics of Nuclear Magnetic Resonance

2.1.1 Magnetic Properties of the Element

Nuclear Magnetic Resonance (NMR) is a spectroscopic method to observe the behavior of any substance when exposed to electromagnetic radiation. Magnetic property of any matter is determined by the spin of basic particles like protons, electrons and neutrons. Each particle has a ½ spin either in positive or negative direction. The Nucleus is comprised of neutrons and protons and has zero net magnetism when protons and neutrons are equal in number. For imaging of the living tissues by MR signal, some important isotopes, present in tissue composition, like ^1H, ^{16}O, ^{17}O, ^{19}F, ^{23}Na, ^{31}P are

taken to consideration [6]. Out of them, ^{1}H has the highest magnetic moment, gives larger signals and it is abundantly present in the tissues. As it has only one charge particle (proton), the spin of the proton can be considered as the spin of the whole nucleus and therefore, the proton is the key particle for the medical MR imaging. The protons according to their spins align in either in the same or in opposite direction of the applied magnetism.
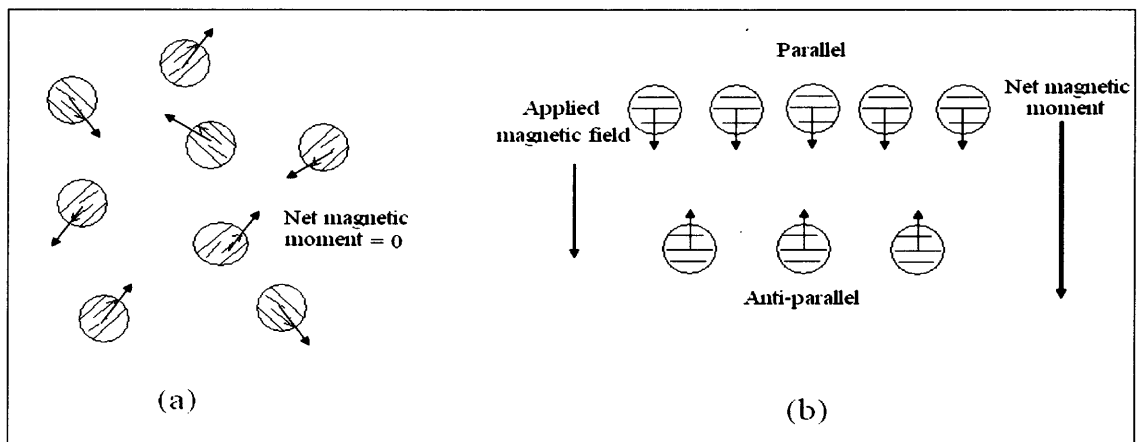
Figure 2.1 Spin characteristics with and without applied magnetic field. (a) Individual spins aligned in random directions in absence of magnetic field and hence no net spin. (b) Spins aligned in either in the same or opposite direction of the applied magnetism and therefore generating net magnetic moment in the direction of applied magnetic field [7].

In absence of external magnetic field, the particle alignments are in random direction due to external thermal energy and inhomogeneity and thus the net spin becomes zero (Figure 2.1 (a)). Permanent magnets are the exceptions in this case as they always have more spins aligned in one particular (either parallel or non parallel) direction. When any object is placed in the magnetic field, its internal magnetism either opposes or gets attracted (as shown in Figure 2.1 (b)) to it.

Depending on the magnetic susceptibility, there are three kinds of magnets: paramagnetic, diamagnetic, and ferromagnetic. Diamagnetic has weak susceptibility which causes to oppose the magnetic field. Paramagnetic is opposite of the diamagnetic which has weak positive attraction forces. Ferromagnetic materials have strong inclination to the magnetic field and some of them are themselves permanent magnets.

When placed in the magnetic field, protons also experience the torque which causes precession and makes that proton wobble around the magnetization vector (Figure 2.2). The relationship between precession frequency (ω_0) and the magnetic field (B_0) is given by larmor equation (Equation 2.1).

$$\omega_0 = \gamma B_0 \qquad \text{or} \qquad f_0 = \gamma B_0 / 2 \pi \qquad\qquad (2.1)$$

Where, γ = Gyromagnetic ratio

ω_0 = precession frequency

f_0 = Linear frequency in MHz (= $\omega_0 / 2 \pi$)

B_0 = Magnetic strength in T (tesla)

The protons precess in parallel (lower energy level) and antiparallel (higher energy level) direction canceling out each other and thus the net magnetization vector remains in the direction of the applied magnetic field. When an RF (Radio Frequency) pulse is give to these precessing particles, they absorb energy and start precession from lower energy level to higher energy level. As this disturbed system goes back to equilibrium it releases the energy in form of an RF pulse which is the MR signal carrying the information about the state of that particular proton. Under the application of 1 Tesla of magnetic field, precession frequency of proton (^{1}H) is 42.58 MHz.
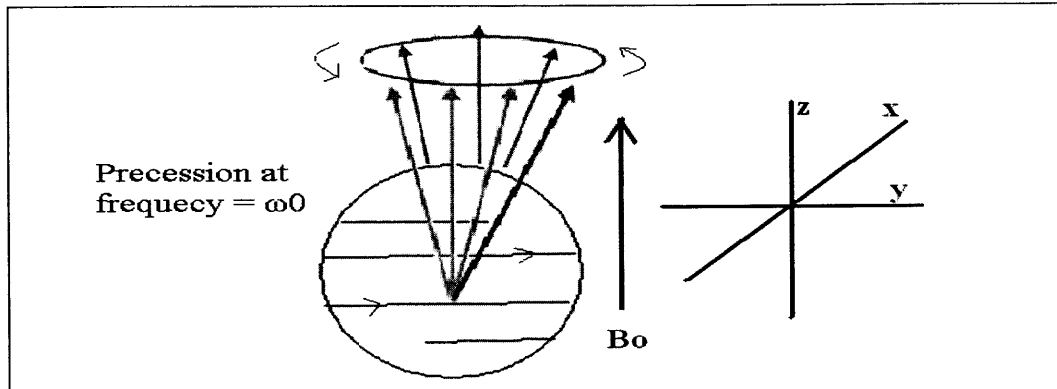
Figure 2.2 Proton's precession about its axis at angular frequency ω_0.

Conventionally, Bo is applied parallel with the z direction of the spinning proton, as shown in the Figure 2.2, which is perpendicular to x and y direction. In the absence of RF pulse, the net magnetization vector (M_0) remains in the z direction which is called longitudinal magnetization vector (M_z). M_{xy} is the transversal magnetization vector which is at 90' from M_z [7].

2.1.2 Important Terms Related to MR Signal

Resonance

Resonance occurs when an RF pulse is applied to the precessing protons and its frequency matches with the precessing frequency. The frequency at which resonance occurs is called the Larmor frequency. If RF pulse frequency does not match with the precessing frequency, the resonance does not occur. At resonance, the magnetization vector M_0 flips from M_z and tries to align with M_{xy}. When Mo returns back to equilibrium it releases RF signal which is proportional to the number of protons transferred from parallel to anti-parallel direction. The flip angle θ can be found using Equation (2.2).

$$\theta = \gamma \, B_1 \, t \qquad (2.2)$$

Where, t = Duration of RF pulse application
B_1 = Magnetic field of RF pulse

From Equation 2.2, it can be seen that θ is directly proportional to time t. If the magnetization vector (M_0) is needed to be flipped at 180', the RF pulse should be applied for double duration than for 90'. Sometimes for faster imaging, smaller angles are chosen [7].

T2 Relaxation

The application of 90' RF pulse flips M_0 to be aligned with M_{xy} and when it returns back to M_z, damped sinusoidal signal is induced by an antenna receiver coil. This damped signal is also known as free induction decay. The decay manner of signal is due to intrinsic inhomogeneity of the tissue which causes the loss of coherence of the spins. This exponential decay can be represented by the below equation.

$$M_{xy}\,(t) = M_0 \, e^{-t/T2} \qquad (2.3)$$

Where, t = instantaneous time
M_{xy} (t) = Transverse magnetization at time t
M_0 = Transverse magnetization at time t=0
T2 = Decay constant (time elapsed between peak M_{xy} and 37% of peak M_{xy})

T2 decay depends on the tissues' molecular properties. T2 decay is shorter for liquid molecules because motion of the molecules makes the dephasing process faster. It also depends on the molecular size. The shorter T2 can be expected for larger molecules. T2 can also be decreased by inhomogeneity of the main magnetic field (B_0) and this decay is known as $T2^*$ [7].
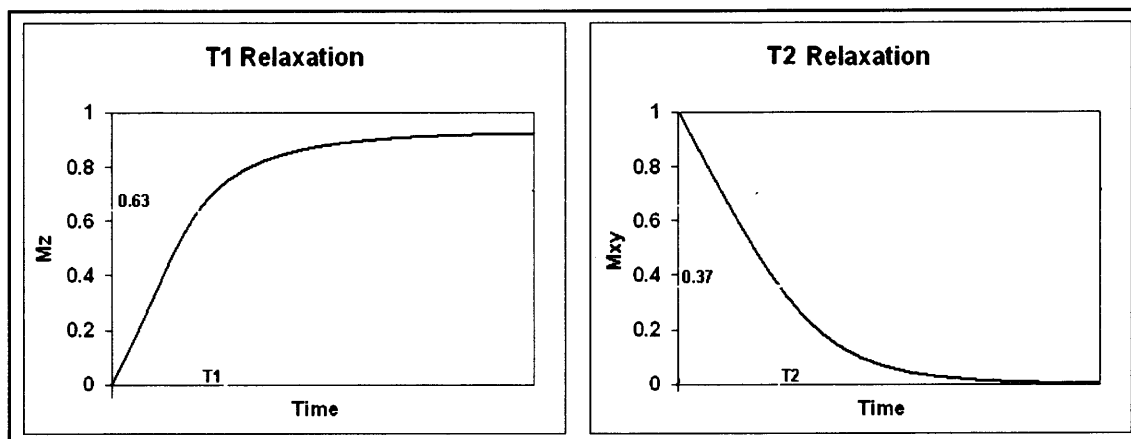
Figure 2.3 T1 and T2 relaxation curves.

T1 Relaxation

The T1 relaxation is time during which the longitudinal magnetization returns back from zero (in case of 90' pulse) to maximum amplitude. This time is not the same as T2 relaxation as both terms are independent. In fact, T2 relaxation generally occurs faster than T1 relaxation. T1 relaxation is also known as spin-lattice relaxation as it depends upon the spin interaction with the molecular properties. The rephasing of the spins can be explained using the Equation 2.4.

$$M_z(t) = M_0(1 - e^{-t/T1})$$ (2.4)

Where, $M_z(t)$ = Longitudinal magnetization at time t
         T1 = Decay constant (time required to reach 63% of maximum M_z)

The T1 relaxation varies with tissue properties. Very small molecules rotate very quickly and thus they give very less potential of resonant frequencies while large molecules rotate slowly and do not give any useful resonant frequency [8]. Medium sized molecules like fat and mucous fluids yield better relaxation and hence exhibit the shortest T1 [7].

Time of Echo (TE)

The echo signal is generated by giving 180' RF pulse after the initial 90' pulse. The echo time will be the twice the time kept between 90' pulse and following 180' pulse. The 180' pulse again rephases the spins and generates the echo of the previous decaying signal. This concept can be well understood from Figure 2.4.
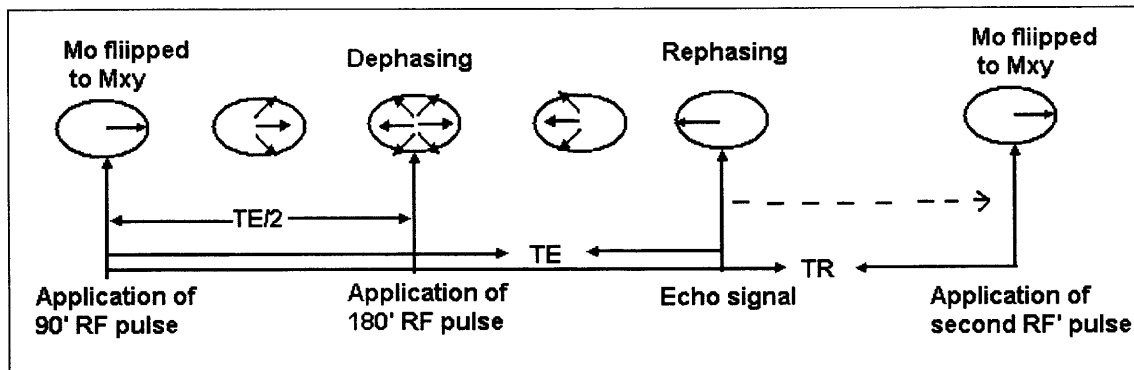
Figure 2.4 TE and TR intervals. The echo signal is generated by giving 180' pulse at TE/2 time after initial 90' RF pulse. Another 90' pulse is given after TR time which generates new FID which will be slightly lesser in the amplitude [7].

When 90' pulse is given, it immediately makes the spins rephase and emit the MR signal. It can be inconvenient to apply RF pulse and receive the MR signal at a single time. The echo signal is helpful because it generated the replica of the decay signal but adds some delay after 90' pulse application [7].

Time of repetition (TR)

Time of the repetition is the duration between two 90' RF pulses. The TR is generally set that the new 90' pulse occurs before complete recovery of Mz and hence the following MR signals are slightly smaller than the very first FID. The second MR signal and

following MR signals will be same in amplitude as tissues become partially saturated during first RF application and remain so during rest of the scanning [7].

2.1.3 Types of NMR Images According to Image Contrast

T1 and T2 Weighted Image

T1 weighted images can be acquired by adjusting TR and TE values and thus eliminating the effects of T2. This way, the major contrast of the image is only due to different individual T1 values of different tissues. To eliminate the effects of T2, TE is kept relatively short and to enhance T1 characteristics, TR is also kept shorter. For T2 weighted images, the TR and TE are selected such that effects of T2 relaxation can be enhanced. Generally, TR and TE values are kept longer to get T2 weighted images.

For example, T1 and T2 relaxation curves for fat, white matter gray matter and cerebral spinal fluid (CSF) are as given in Figure 2.5.
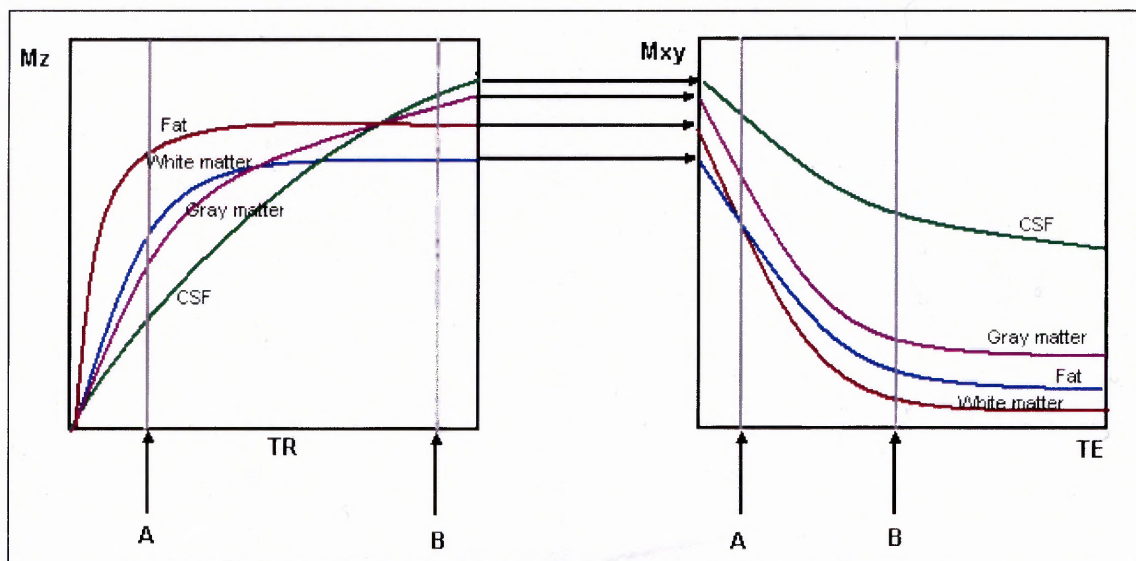
Figure 2.5 Longitudinal recovery (T1 relaxation) and Transversal decay (T2 relaxation) curves for tissues of fat, white matter, gray matter and CSF. Points denoted by 'A' and 'B' are selected values of TR and TE to get T1 and T2 weighted images, respectively [7].

From Mz vs. TR graph, it can be seen that at shorter TR (point 'A') these tissues have greater difference of T1 values and at longer TR (point 'B') they have less discrimination. Therefore, for shorter TR can be selected to enhance contrast due to T1 and longer TR can be selected to inhibit T1 effects. Same concept can be explained from Mxy vs. TE graph for effects of T2 relaxation [7].

Proton Density Weighted Image

As the name suggests, in this type of images, the image contrast depends on the number of spinning protons present in the tissue rather than T1 or T2 characteristics. The TR is kept longer to eliminate the influence of T1 constants and TE is kept shorter to discard T2 weighting. The image contrast is relatively poor in proton density weighted images. Tissues with lower proton density like air and bone yield smaller signals and show up as dark areas in the image while, hydrogenous tissues like fat and CSF yield larger signal and thus show up as bright regions [7].

2.2 Geometric Orientation of MR Signal

Slice Select Gradient

The slice select gradient (SSG) is used to select the slice of desired thickness and position. This gradient is provided in the axial direction i.e. z-direction of the subject. This gradient is given as linearly varying field intensity of RF pulse over finite region. The bandwidth of the RF pulse can be used to determine the width of the slice. According to larmor equation, field intensity is proportional to precession frequency and thus by providing bandwidth of RF pulse, the protons in specific region precess which experience

the resonance. The narrow bandwidth excites protons of narrow slice and vise versa. The slice thickness also depends upon the field strength. The higher strength produces a thinner splice. The slice select gradient determines the specific region to be scanned [7].

Frequency Encode Gradient

Frequency encode gradient (FEG) is applied along the x-direction of the subject. The gradient is given as changes of precession frequency which is null at center of slice, higher at the right side and lower on the left side. The positions column by column i.e. from left to right are differentiated according to linearly varying frequency values [7].
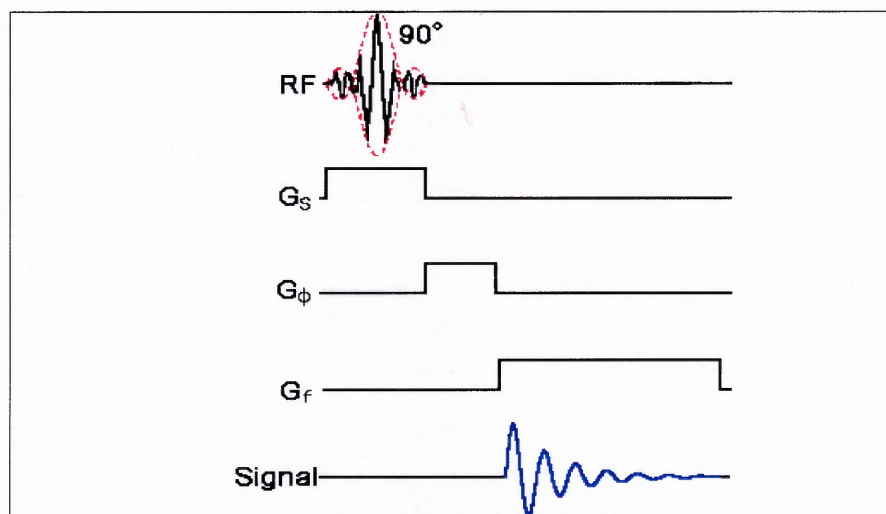
Figure 2.6 The sequence of three gradients applied for the localization of 90' RF pulse [9].

Slice encode (G_s) is applied at the same time of RF pulse to select the slice. Then applied is the phase encode (G_φ) to enter phase shift and after turning off the phase encode, frequency encode (G_f) gradient is applied [9].

Phase Encode Gradient

Phase encode gradient (PEG) determines the y-direction of the image hence helps to change the signal row by row. This gradient is provided after the application of RF pulse. The phase gradient changes the frequency of the precessing protons and when it is turned off the protons return to original precession frequency but with different phases. This gradient changes the phase at each TR according to desired number of voxels. The phase shift is null at the center, lagging in negative direction and progressing in the positive direction [7]. The sequence of these gradients in accordance with 90' RF pulse is shown Figure 2.6.

2.3 MRI Instrumentation

The simplest MRI instrumentation includes a magnet, RF coil, Gradient coils, consol to control gradients and pulse sequences and an image construction processor. More facilities can be added to the instrument as per requirements. The most important part of this instrument is the magnet which generates magnetic field B_0.

2.3.1 Magnet

The most important criterion in selecting a magnet for resonance imaging system is its field strength. Normally, for MRI machine, the magnetic field strength ranges from 0.2T to 3 T. There are basically three types of magnets used in MRI instrument which are permanent magnet, resistive magnet and superconductive magnet.

Permanent magnets generate magnetism without any external excitation. These magnets are large and heavy and can not generate higher magnetic strength. They are

relatively cheap and easy to maintain. The major disadvantage of permanent magnet is that it can not be turned off in case of emergency.

Resistive magnets are made using core and a current carrying coil wrapped around it. When the current is passed through coils, magnetism is produced in the core. They need constant electric supply and can be easily turned off. The heat dissipation is higher in these magnets and thus they need cooling systems. The main disadvantages are higher cost and poor uniformity of the field. It generates around 0.1 to 0.3 T of magnetic field.

Superconducting magnets are most commonly used magnets for MRI. They are similar to resistive magnets as they also have current carrying coils around a core but these coils are continuously submerged in coolants (for example, liquid helium) and thus they reduce the chances of heat dissipation and also alleviate the resistance of the coil. Due to less resistance, the current increases in the coil and higher magnetic field is produced using lesser electricity. These magnets are costly due to use of expensive coolants. They can produce 0.5 to 10 T of nicely uniform magnetic field and thus higher image quality can be acquired. Superconducting magnets are closed structure and can be uncomfortable for claustrophobic patients [7].

2.3.2 RF Coil

The functions of RF coils are to generate RF pulses (magnetic field B_1) and to receive the MR signal from the tissues. The magnetic field B_1 is generated perpendicular to the main magnetic field B0. The transmitter and receiver coils can be separated or only one coil can perform both tasks. These coils should be able to produce the resonance. The

distance between the coil and the object determines the field strength. If the coil is placed nearer to the object, it produces stronger field (B_1). The type of the coil is decided from the type of object to be imagined. The SNR (signal to noise ratio) can be a major criterion in selection of coils [7].

2.3.3 Additional Components

The important additional components are gradient coils, shimming coils, consol, image construction hardware and software. Gradient coils are placed inside the drum of the main magnet and they are excited as explained in the section 2.2.1. Shimming coils are used to adjust the magnetic field B0 and to maintain the homogeneity of B0. The consol contains the controls for gradient coils, RF coils, patient table, etc. The image construction tools are used to construct the image from received MR signals and to adjust the image parameters like brightness and contrast [7].

2.4 Functional Magnetic Resonance Imaging (fMRI)

The MRI image is a snap shot of the anatomy of the brain which helps viewing different regions of brain and their structure. Only a single image can be sufficient for this type of imaging. The functional MRI image helps to observe physiological changes occurring in different areas of brain over time. It collects many images which are useful to track changes in reference to the experimental stimulus. The fMRI produces signal changes according to the BOLD (Blood-Oxygen-Level Dependent) signals received from the brain as explained in the below section [10].

2.4.1 The BOLD Response

FMRI is the technique that measures cerebral blood flow, and cerebral blood volume changes in the brain while performing different various tasks and control conditions. The increased neural activity following a task/stimulus elevates the need for Oxygen supply, which results in increased blood flow to the activated region. The cerebral blood flow contains hemoglobin which has diamagnetic (negative magnetic susceptibility) properties when oxygenated but has paramagnetic (positive magnetic susceptibility) characteristic when deoxygenated [10]. The elevated oxygen consumption changes the hemoglobin-oxygen (HbO_2) level and therefore the observed MR signal. This change in MR signal mechanism is known as BOLD (Blood-Oxygen-Level Dependent) response. Hence, for different physiological states, images with signal changes occurring in the brain can be acquired [5].

2.4.2 Experimental Design

The experimental design of fMRI study is the practice of using stimuli in conjunction with the scanning to acquire satisfying results for the given hypothesis. For most of the fMRI researches, two kind of experimental designs namely the block design and event-related design are typically used. Both methods have advantages and disadvantages with them and ultimately the selection of them depends on the type of the study and the hypothesis to be tested. For example, block design is appropriate for the finger tapping experiment as it has two distinct responses for "Task" and "Rest" states while the experiment involving watching a movie can need event related design as brain response changes continuously [10].

Block Design

In block design, the stimuli are presented to the subject for blocks for several seconds. The brain response is assumed to be similar or constant over a single block. The transition from one block to other triggers similar fMRI signal changes and the temporal data can be used to study brain response for each individual block. Many times the task block is followed by a control (rest) block which helps the MR signal returning to the baseline. The duration of the task block is an important criterion. Very short block can limit the subject's fMRI signal response and can also takes some time to be stabilized to one level. Longer blocks which significantly improves signal detection, can also be disadvantageous due to motion artifacts and in some cognitive tasks when subject starts learning and being indifferent to the stimulus. Some tasks like breath holding can be difficult to last for longer time and that limits the block duration. Block designs can be created and correlated to the fMRI outputs very easily but might not suitable for some studies [10].

Event-Related design

Event-related designs are especially for the short term/constantly changing neural activities. It is a sequence of many different tasks that take place for shorter durations and time between two stimuli can be random. This method provides higher flexibility for the timings of the tasks, and can control for various cognitive process including attention, learning, and habituation. It is advantageous over block design as it can measure the response for many stimuli in a single run. Thus, while block design can detect processes, event related design can detect single events. It can be also helpful to find the pathway of

connectivity between different regions of the brain. Sometimes the signal gets distorted because of motion or respiration and it is very hard to detect whether the signal is changed due to different task or the artifact [10].

2.4.2 FMRI Artifacts

The main causes of artifacts in fMRI signal are thermal noise, inhomogeneity of the magnetic field, external noise, head motion, physiological activities like respiration and pulsatile blood flow and neuronal activates which are not due to the stimulus [30]. The magnetic inhomogeneity can cause difference in precessing frequencies of the proton and hence affect the spatial resolution of the image. Signal change due to head motion and physiological activities are not uncommon and play a major role in spatial and temporal artifacts. For certain tasks, it becomes very difficult to distinguish between signal changes due to task and due to motion [10].

In summary, the functional magnetic resonance imaging is a useful imaging technique which provides not only the picture of the inside of the brain but provides the information about ongoing process of the different regions of the brain. It involves no harmful chemicals or radiation and gives better image resolution than PET or CT scan. It is more expensive compared to other imaging modalities and that is the sole reason that it is not being used for larger population of the world. The careful experimental design can give clear representation of the brain response to the particular stimulus. There are few artifacts in fMRI but they can be minimized with the better design of MR instrument.

CHAPTER 3

DATA ANALYSIS

Data analysis plays a crucial part for all fMRI experiments to prove the underlying hypothesis to be tested. It also plays an equally critical role in pre-processing and feature selection prior to pattern recognition. It could be very hard to get accurate classification results without performing this step. Data Analysis consists of various stages including motion correction, histogram study and feature selection techniques. Motion correction is generally the first step to be performed which helped to remove the motion artifacts and align the corresponding voxels of different images to the same dimensions. Histogram study was done to find whether images with different physiological conditions were distinct enough for classification. Feature selection is the most important part which helps to find the multi-voxel patterns for classification. These stages are explained in detail in below sections.

3.1 Motion Correction

Motion Correction is a necessary step to be performed on fMRI images prior to any additional data analysis. The head motion in human subjects is not unusual for a long run of the experiment. This artifact needs to be corrected because it is assumed that each voxel in the image had same dimensional location (x-y positions) through entire scanning and only then voxel to voxel time series comparison is possible. Head motion induced signal changes also are not due to the stimulus but in many cases may be correlated to the stimulus. The best strategy for motion artifact is to prevent the motion

by using cage or some padding to keep the head in stationary position throughout scanning. Motion was not significant with the rats' data because rats were anesthetized during the scanning. There are various methods for motion correction but the most common method is to take one image (usually image at the early time point) as a reference and all other images will be repositioned according to that image. It is usually assumed that head does not deform during the scan and is referred to as rigid body registration [10].

In this study, AFNI (Analysis of Functional NeuroImages) software was used for motion correction of human and rat data sets. It used an arbitrary image from each time series data sets and registered it with every image in the time series. For this study, the reference (base) image was set as the fourth time point in this experiment. The registration algorithm uses a linearized least square algorithm to register all images to the base image. In addition several options like 'fourier' and other interpolations, 'clipit' to clip the volume of each image to match with reference image, 'zpad' to pad with zeros at the edges exist in the algorithm [11].

3.2 Histogram Study

The distribution of the signal intensity within a brain image (or within a single voxel over a period of time) was performed using histogram analysis to find out different intensity thresholds which helped to differentiate the images of different conditions. It is an important step especially for gas mixture data to find out whether the images taken while breathing different gas mixtures were distinct enough to be classified or not. Prior to plotting the histogram, the time series of the data were observed to determine the level

change of the signal for different states. The data were then analyzed to see whether all possible classes were statistically separable from each other using histogram analysis. Threshold values for signal intensities which may help to discern the images can then be determined. These threshold values can then be used to find activation in each of the fMRI images. Consequently, a set of activation maps can be created and compared to discern different conditions based on intensity values.

3.3 Feature Selection

Feature selection is a very important criterion for classification of fMRI images. For the specific stimulation given to the subject, only a small fraction (typically less than 100 voxels) of the brain volume gets activated. These activated voxels are very less in number compared to entire volume of the brain. It is thus difficult to perform pattern recognition on entire images for these small activations, since the overall effect is diminished. So, while performing classification, it is necessary to find out only those voxels which react to the task/stimulation condition.

In this study, feature selection was done in two steps: Masking and statistical analysis. Masking was done using AFNI software to remove the background voxels from brain voxels. This was done because a large portion of the fMRI obtained contains voxels from region surrounding the brain. Specific voxels selection was done in MATLAB using statistical techniques like correlation (for first study), paired t-test (for second study) and ANOVA (for both studies).

3.3.1 Masking

Masking is a useful method to decrease the size of the data by removing the background voxels (voxels which are not included in the brain) and to focus only on those voxels which carry the useful information from the brain. The mask was created using AFNI. There are two possible methods to create the mask using AFNI, one is using automask and the other is creating a mask manually. Automask creates the mask by clipping the data which do not have values above the particular threshold. This clipping level can be selected as per the requirements of the mask size. Mask also can be created manually by simply drawing the boundary around the specific region which needs to be used as the mask [11]. In this experiment, the area of mask was chosen manually. In this study, for both the experiments (finger tapping and gas mixture tasks), the whole brain volume was selected as the mask rather than selecting a particular brain region.

3.3.2 Correlation

Correlation is a simple statistical technique that computes the degree of similarity between two groups. Its value ranges from -1 to 1 where 1 indicates that both groups are identical and 0 indicates no similarity between them. Negative value shows the negative correlation due to one of the signal being out of phase [12].

This statistical technique was used for finger tapping data, where activation had a unique "ON and OFF" pattern. The 'Rest' condition was considered as a lower level response (i.e. 0) and the 'Active' condition was considered as a higher level response (i.e. 1). This finger tapping response can be compared to a pulse cycle of definite duration. The correlation-coefficient matrix was found using MATLAB function "corrcoef". To

find the voxels that responded well for this task, 'Rest' and 'Active' images were considered as different groups. The series of activation and resting images were compared to the reference vector which is shown in Figure 3.1 and the correlation coefficient was calculated on a voxel wise basis for the every voxels in the brain. The number of 1s was assigned same as number of active images and number of 0s were same as number of non-active ("Rest") images.
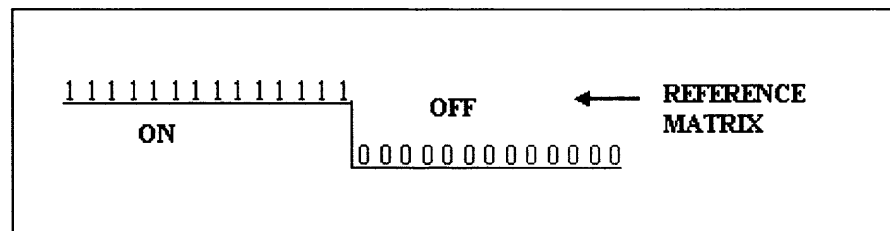
Figure3.1 A reference matrix used for finding correlation coefficient of each voxel for finger tapping data.

Voxel time-series that followed the reference pattern were considered as active and selected. The correlation coefficient gave the measure of similarity in form of values between -1 and 1. To extract the most effective voxels, a threshold value was selected. The voxels having correlation values more than this threshold were chosen for classification.

3.3.3 Paired T-test

T-test is used to find the differences in the means of two different groups. It measures the probability in favor of the provided null hypothesis, which states "The means of two groups are equal". The significance level alpha is generally set to 0.05 and the alternative hypothesis for this case was "The means of two groups are not equal" [13].

The t-test was used to determine significant voxels for gas mixture data. T-test can not be performed on more than two groups and thus t-test was done pair wise. It was performed on every possible pair of images. In this study, for ten different conditions of gas mixture data, total 45 different t-tests were performed. The common threshold value was chosen to select out voxels from each t-test. The voxels which were selected by each t-test were further utilized for pattern recognition.

3.3.4 ANOVA

ANOVA is a widely used statistical techniques for comparing two or more groups. It tests these groups for the equality of means and measures the probability of the null hypothesis, where null hypothesis was stated, "Mean of each group is equal". The alternative hypothesis is true when any two sample means are different. ANOVA computes variation within the groups and between the groups. If the variation within the samples is low and between the samples is high then there is a significant difference in means of these groups [12].

In this study, ANOVA was used to find voxels, whose intensities were distinctly different for various stimuli. This technique was used for finger tapping as well as gas mixture data. Images with different patterns were referred as different groups of ANOVA. In each group same numbers of images were used and ANOVA was performed using MATLAB. With the use of threshold value voxels having higher variability between groups were selected. The threshold value was selected as per the requirement of the desired number of voxels for pattern recognition.

CHAPTER 4

PATTERN RECOGNITION TECHNIQUES

Pattern recognition is the process that identifies the given data (or images) using available prior knowledge about their characteristics. It has wide spread application in various fields including biometrics, space technology, image processing, iris recognition, handwriting recognition, and face recognition [14]. Pattern recognition is one of the applications of classification technique which uses machine learning algorithms. Classification is a statistical method to categorize and cluster existing data according to their distinct characteristics. Today, there are many techniques available to solve classification problems. Neural networks and Support Vector Machines are few such methods. These methods accept datasets (inputs) along with their labels (types of category) for the training of the network. The training process enables the network to classify the datasets as per their unique labels and when the network is given the test data; it determines the category of this data according to prior knowledge gained by training. The classification accuracy depends upon type of the algorithm used, the type of datasets, and the underlying noise sources. If the datasets are distinct and linearly separable, then simple linear algorithm is sufficient but if the datasets are overlapping and have very few changes compared to overall data, then more complex classification tools are needed. The fMRI images show very less overall variation for different conditions and thus their classification is a challenging task. The following sections explain different classification tools including neural networks and LS-SVM (Least Square Support Vector Machine).

4.1 Neural Networks

Simon Haykin (1999) has defined neural network as: *"a massively parallel distributed processor made up of simple processing units which has a natural tendency to store experimental knowledge and making it available for use."* [15]. The Neural network is architecture of multiple artificial neurons semi or fully connected to each other. The concept of artificial neural network is inspired from biological neural connections and their functions [13]. The biological neuron has dendrites to receive the inputs, cell body to process the inputs and an axon to deliver the output to the next neuron. The axon is connected with dendrites of other neurons through synapse and that way the network is created. The brain contains millions of these neurons complexly interconnected. Each neuron generates a signal when gets activated i.e. its total input value goes higher than the set threshold through electrochemical process. Same way, the artificial neuron is the processing unit of the neural networks with many inputs and one output. The artificial neuron receives inputs from connections specified with distinct weight vectors that are similar to synaptic strengths. The negative weight values indicate the inhibitory function of the brain neurons.
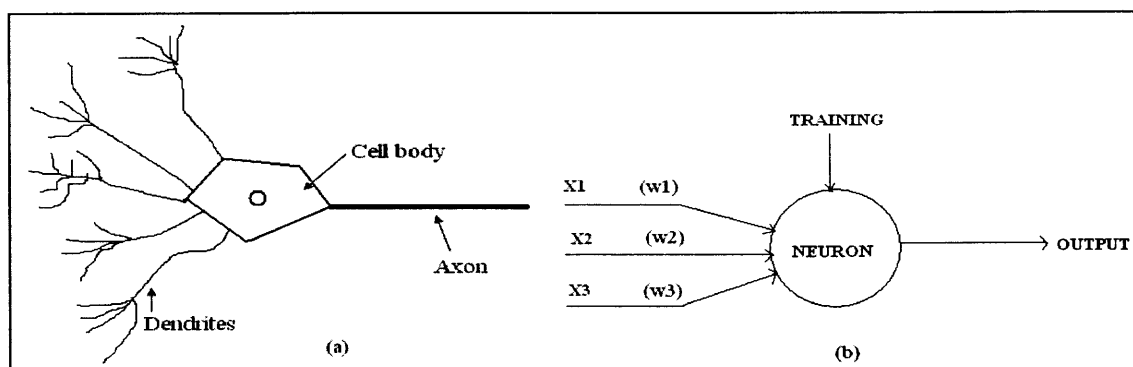
Figure 4.1 (a) Biological neuron and (b) simple artificial neuron architecture.

The artificial neuron is the smallest unit of complex artificial intelligence (AI) system whose basic function is learning. The learning process can be supervised (i.e. target values are provided) or unsupervised (no information about target values are provided). The learning process updates the neuron's function. It multiplies the incoming inputs to the corresponding weight vectors and adds the bias if necessary. Bias is the threshold value which is generally negative to subtract common value from the sum of the inputs. This procedure can be understood by Equation 3.1.

$$s = \sum_{i=1}^{n} x_i w_i + B \qquad (3.1)$$

Where, n - Number of neuron inputs
x_i - i-th input value
w_i - i-th weight vector
B - Bias

This set of inputs is then given to the transfer function. This transfer function (f) can be linear, hard limit (step function), logarithmic sigmoid, saturating linear or compet (competitive transfer function - "winner takes all" principle) [16]. The output of the neuron will be the output of this transfer function.

$$Y = f(S) \qquad (3.2)$$

Where, f - Transfer function
Y- Output of a neuron

Number of layers in the neural network determines the complexity of the network. The two layers (inputs are not considered as a layer), fully connected, feed forward (unidirectional flow of data from inputs to output) network is shown in the Figure 4.2. The middle layer is also known as a hidden layer.
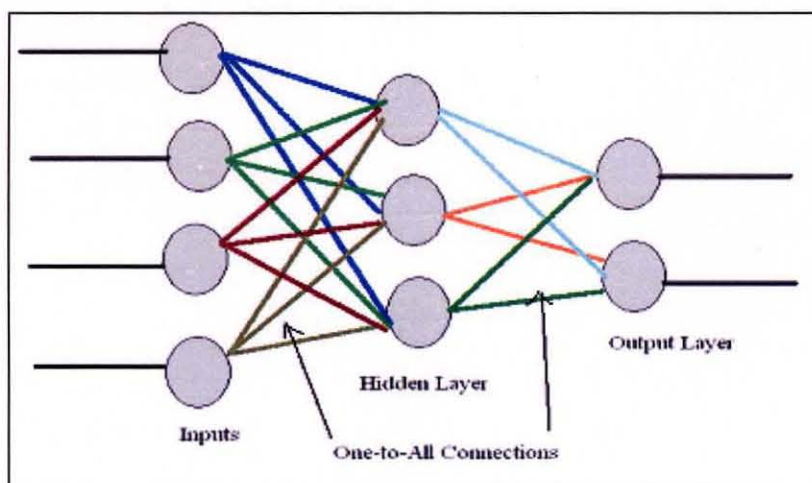
Figure 4.2 Two layer neural network with multiple inputs and multiple outputs.

For binary classification, there are number of predefined networks available like perceptron and learning vector quantization. The perceptron network does not have any hidden layer and thus is not able to classify the non-linear problems while learning vector quantization networks gives very effective classification for non-linearly separable classes.

4.1.1 Perceptron Network

The perceptron is a single layer, feed-forward network and is used to solve simple classification problems like binary classification [15]. It takes multiple inputs and target values for the training process. By training this network, a linear decision boundary can be created. When a new set of inputs is tested for this trained network, the network classifies it according to this boundary. This can be explained by a simple AND function. The truth table shows inputs P1 and P2 and output T corresponding to them.

Table 4.1 Truth Table for 'AND' Function.

P1	P2	T
0	0	0
0	1	0
1	0	0
1	1	1
0.9	0.9	?

The perceptron network was trained using first four inputs and target output values (either zero or one). According to these values, it created a decision boundary to separate two classes. The plot is showed in Figure 4.3 where 'o' symbolizes class-1 and '+' shows class-2 inputs. Then, this trained network is simulated for fifth input set ([0.9 0.9]) and it is correctly classified as class-2 according to this decision boundary. The perceptron network can be trained again and again for new input and target values and it changes its weight vectors and thus the boundary position each time.
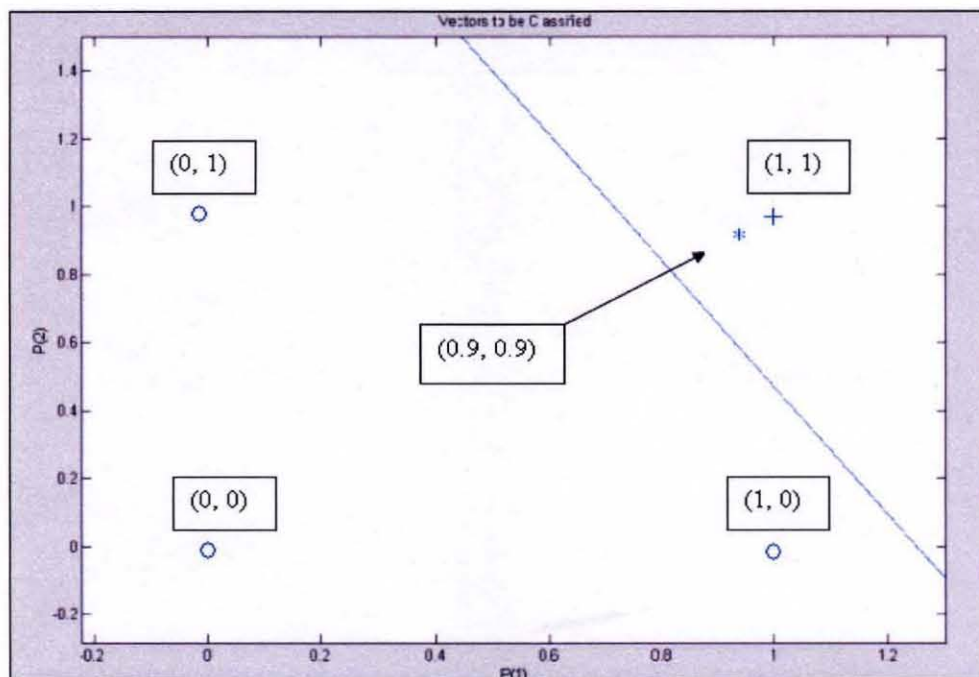
Figure 4.3 Plot created for perceptron classification of 'AND' function.

4.1.2 Learning Vector Quantization Network

Learning Vector Quantization (LVQ) was invented by Teuvo Kohonen [15]. It is a feed forward, two layers, fully connected supervised network. The first layer uses the compet transfer function and the second layer has linear neurons. None of the layer has biases [16]. LVQ works using a learning process which includes updating of weight vectors during each training procedure. It doesn't create common decision boundary like in perceptron. Instead, class boundaries are built piecewise-linearly as segments of the mid-planes between neighboring classes and these boundaries are modified during each learning process. If the inputs are very similar then it is not possible to create distinct regions for them.
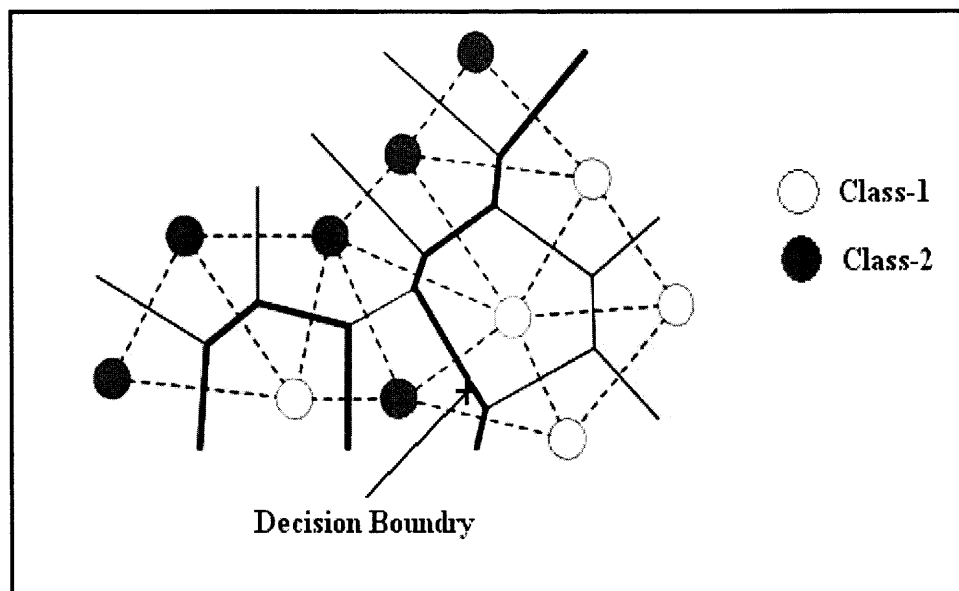
Figure 4.4 Classification using piecewise-linear boundary for learning vector quantization networks [17].

To test this trained network, new unknown data is given and is classified according to the distance from the defined regions. Generally, the Euclidean distance is

used for comparison between an input vector and the class representatives. The class of the new data will be decided according to which region is the nearest. The less distance suggests the higher resemblance [17].

4.2 Least Square Support Vector Machine

Support Vector Machines were introduced by Vladimir Vapnik. They are used for classification and regression tasks. They prepare a network which can be trained using the data and their assigned labels and this network is then used to perform the required task. To perform the classification task, support vector machines try to make a hyperplane in the space for available inputs and their labels. The data are separated according to their class and put in separate regions away from each other as much as possible. While new dataset is fed for testing, SVM try to find distance of new data set from the defined regions. According to this distance the class of new dataset can be predicted [18].

LS-SVM (Least Square- Support Vector Machine) is derived from the original SVM. It is based on the background of statistical learning process. It is proved more competent for especially multi-class classification. LS-SVM is used widely these days for solving classification problems. It is very efficient for nonlinear classes and takes less time for training.

For classification process, it takes certain parameters together with input data and target values. They are type of the model (function estimation or classifier), regularization parameter γ, kernel parameter σ, and kernel type. In the present research,

'Classifier' for binary classification and 'Function Estimation' for multi-class

classification were chosen as model types.
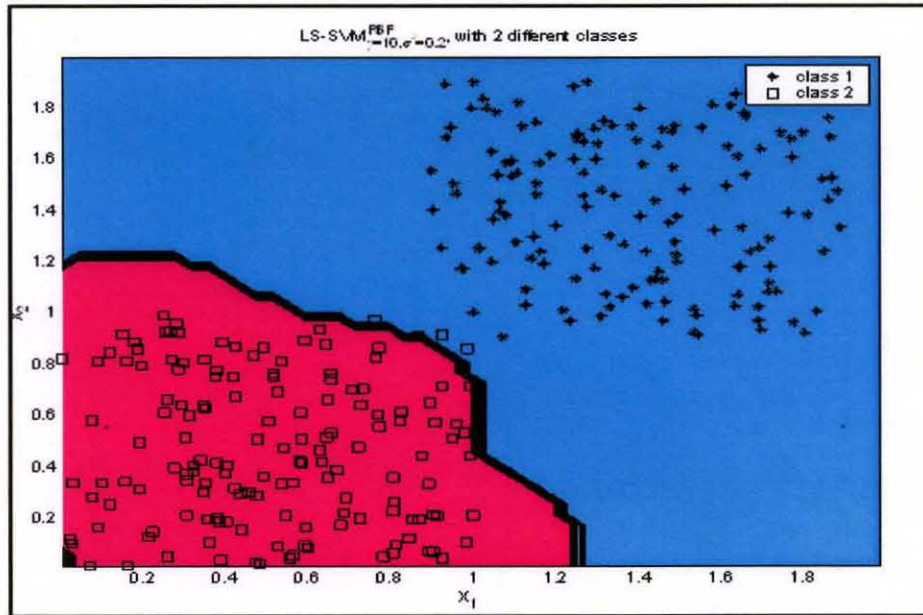
Figure 4.5 Example of binary classification using LS-SVM. Magenta shows class-1 region and cyan shows class-2 region. Black thick boundary is the classification boundary created by the LS-SVM model.

For kernel selection, there were basically three choices: linear, polynomial and

RBF (Radial Bias Function) kernel. Accuracy for classification output is so much

dependent on regularization parameter γ and kernel parameter σ [19]. The calculation for

these parameters is very complex and hence, generally these values are found by

performing grid search. The grid search is also a tedious job but that is relatively simpler

way to find these parameters.

In first step of grid search, wide range of rough grid values is chosen according to

the dimension of the inputs. The gird value selection depends on the user and as both

parameters are independent the grid search is simpler.
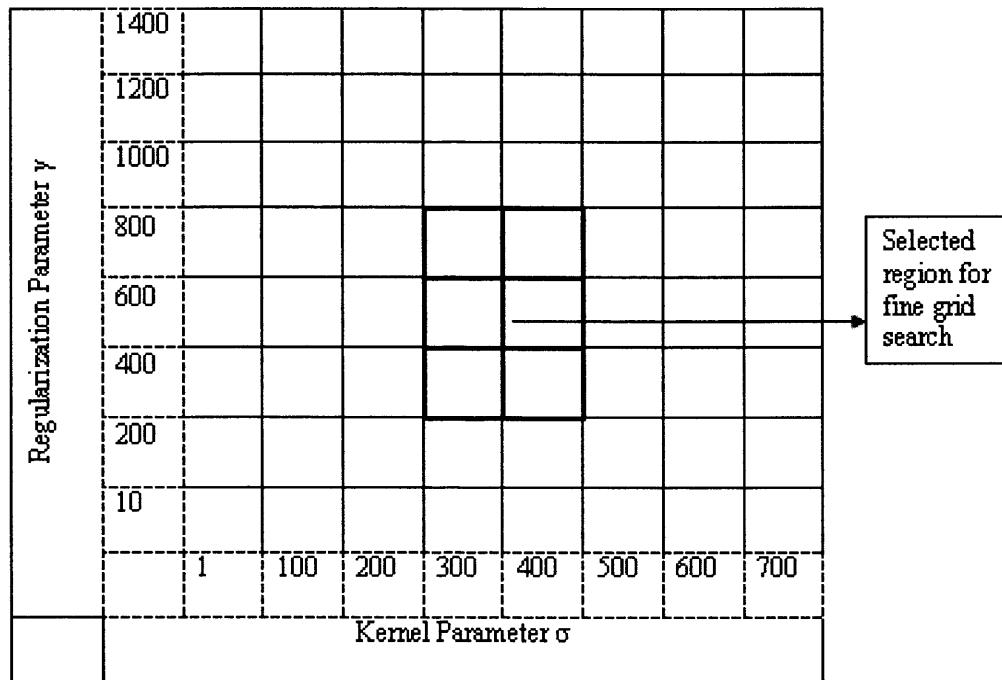
Figure 4.6 Example of grid search method to find the values of regularization parameters.

After running the algorithm for each set of grid values, the particular region of the grid is selected where the better results are found. Second step is the fine grid search, where the procedure is repeated on the selected section and the most appropriate values of γ and σ are estimated for training LS-SVM model [20]. For each experiment with new dimensions of inputs, the new grid search should be performed to obtain highest output accuracies.

CHAPTER 5

METHODS AND MATERIALS

5.1 Finger Tapping Data

5.1.1 Subjects and Data acquisition

In the experiment of finger tapping task, four (three male, one female) healthy subjects who aged between 20 and 30 were participated. Written consent was obtained from each of the subjects prior to scanning. Subjects were paid on an hourly basis for their time and the experiment was approved by the local Institutional Review Board.

Each subject was asked to perform a finger-tapping task as per the instructions presented on a visual screen. The subjects were asked to tap their both fingers when images were presented on the screen and to stop when they blank screen appeared. The duration for finger tapping was 20 seconds followed by rest period of 20 seconds. The total duration of scanning for each subject was 180 seconds (3 minutes).

The scanning was done using a 3T Siemens Allegra (Ehrlagen, Germany) imaging system. The imaging system was equipped with a three axis balanced torque head gradient coil and a shielded end cap quadrature transmit/receive birdcage radio-frequency coil. Volunteers were positioned supine on the gantry with the head in a midline location of the coil. To reduce motion artifacts, foam padding was placed between the forehead and the coil. In our experience, foam padding considerably minimizes head motion and allows only small motions. Each scanning session began with acquisition of high-resolution (256x256) anatomical T1-weighted axial images. Based, on the high-resolution

images, several axial slices covering the entire sensorimotor cortex and its associated areas were chosen. For this study, seventeen axial slices echo-planar images were found to be adequate to cover the entire sensory motor cortex. Echo-planar images were obtained using the following imaging parameters: TR=1000ms, flip angle=90°, TE=27 ms, slice thickness = 5 mm, FOV = 22cm x 22 cm, and Matrix size = 64 x 64. This resulted in a spatial resolution of 3mm x 3mm x 5mm pixel. During each run, 139 echo planar images were collected for further data analysis.

5.1.2 Pattern Recognition

AFNI was used to analyze the fMRI data sets obtained. Motion correction was done for each subject to ensure that all images were in same position. Feature selection was the next step to be performed. Both correlation and ANOVA were used as feature selection techniques. For correlation eight 'Active' and eight 'Rest' images were used which were not included in the test data set. The reference shown in Figure 4.1 was used to find the correlation between two categories using MATLAB function "CORRCOEF". The probability threshold was set and voxels having higher probability than these were selected. For ANOVA, eight 'Rest' images were taken as one group and eight 'Active' images as the second group. The null hypothesis was tested for these two groups and found the probability values. This was done using MATLAB function "ANOVA1" which is one way ANOVA method. Voxels with the probability threshold or less were selected. Logical 'AND' function was performed to find common voxels selected by both techniques and these voxels were used for the training of the network.

For binary classification, there are many methods available. In this study, LVQ network and LS-SVM were used. Generally for any classification task, total number of datasets is divided in two equal groups. One group is used for training and the other group is used for testing. In the present experiment, the datasets were divided in two groups for training and testing by approximate ratio of 60:40. The 'Rest' images were assigned as class-1 and 'Active' images were assigned as class-2. For LVQ network, neural network toolbox provided in MATLAB 6.1 was used. The weights of the network were updated by training it for each new set of images. The trained network was simulated to find out whether the image is active or at rest.

For classification using LS-SVM, LS-SVMlab Toolbox (version 1.5) created by Research Council, KULeuven university-- ESAT - SCD-SISTA was used. Regularization parameters were established according to the data size. Unlike LVQ, LS-SVM was trained in a single session using all input test images simultaneously. This trained network was then tested using the unknown images to predict the state.

5.2 Gas Mixture Data

5.2.1 Animal study and Data acquisition

For this study, four male Sprague-Dawley rats were used. For the scanning, they were anesthetized and their body temperature was maintained at 37.0 ± 0.5' C. They were ventilated mechanically with air. A paralyzing agent was given in the beginning to them to stop sudden breathing during scanning. Mean arterial blood pressure was checked continuously and blood gas samples were taken before and after the scans and analyzed. All rats were given room air (21% Oxygen), 100% Oxygen, Carbogen (95% Oxygen+5%

CO_2), 2 % CO_2 and 5 % CO_2 at regular intervals. These gas mixtures were given for 15 minutes each following by 20 min ventilation with air + 30% Oxygen. MRI scanning was started 5 minutes late every time after starting of particular ventilation. Total experiment duration was 3 hours for each animal. Scanning was done using Bruker Medscape 3T/60 cm imaging system. An RF bird-cage coil with the length of 0.5 cm and diameter 3.8 cm was used to acquire the data. The rat was secured to RF coil by bite bar to minimize the motion artifacts. First anatomical coronal images were taken using RARE (Rapid acquisition relaxation-enhanced) sequence with TR=1 sec, TE=19 ms, 256*256 matrix and 3.5 cm of field of view. Then taken were fMRI images using TR=2 s, TE=27.2 ms, 64*64 matrix, 2 mm of slice thickness and bandwidth of 125 kHz. Total 180 images were acquired per each of total three slices. Images were collected for 60 s while breathing, alternating with 30 s of Breath hold in three epochs.

In this study, images were collected for ten different conditions, for five different gas mixtures at rest (normal breathing) and at breath hold. They are shown Table 5.1.

Table 5.1 Ten Different Conditions for Gas Mixture Data

Gas mixture	At Rest	At Breath Hold
Room air	Class 1	Class 6
2 % CO_2	Class 2	Class 7
5 % CO_2	Class 3	Class 8
Oxygen	Class 4	Class 9
Carbogen	Class 5	Class 10

5.2.2 Pattern Recognition

The first step of the procedure was to set up a pattern made up of selective voxels. To find these voxels, two statistical techniques: pair wise T-test and ANOVA were used. The MATLAB function "TTEST" was used with ALPHA = 0.05. The significant voxels were found and used for pattern recognition. ANOVA was performed on sets of five images of ten different classes using MATLAB function "ANOVA1". The probability values for each voxel in support of null hypothesis were calculated. Threshold value for probability was set and voxels which showed probability less than this were selected as featured pattern for training and testing.

For pattern recognition task, all possible images for every class were taken. It was hard to set a ratio of images for training and testing because each category had different number of images. The LS-SVM was used as classification toolbox for this multi-categorical data. The parameters of LS-SVM were discussed and selected to get the best results. Appropriate values for regularization parameter (γ) and Kernel parameter (σ) were found by 'Grid Search' method. Training sets i.e. different classes were assigned labels of equal intervals to give same weight to all classes. These labels were from 100, 200, . . , 1000 for ten different classes. The LS-SVM network was trained using these labels and training datasets. This trained network was simulated for test images for pattern recognition. For LS-SVM, it is hard to give crisp output values like 200 or 400. Instead, it gives values nearer to particular label and according to this output value the class type can be determined.

CHAPTER 6

RESULTS

6.1 Results of Finger Tapping Data

6.1.2   Histogram Study

As it can be seen from time series of finger tapping data (Figure 6.1 (a)), the two states "Rest" and "Active" were distinct. The ideal response for finger tapping task is shown in red.

(a)   (b)
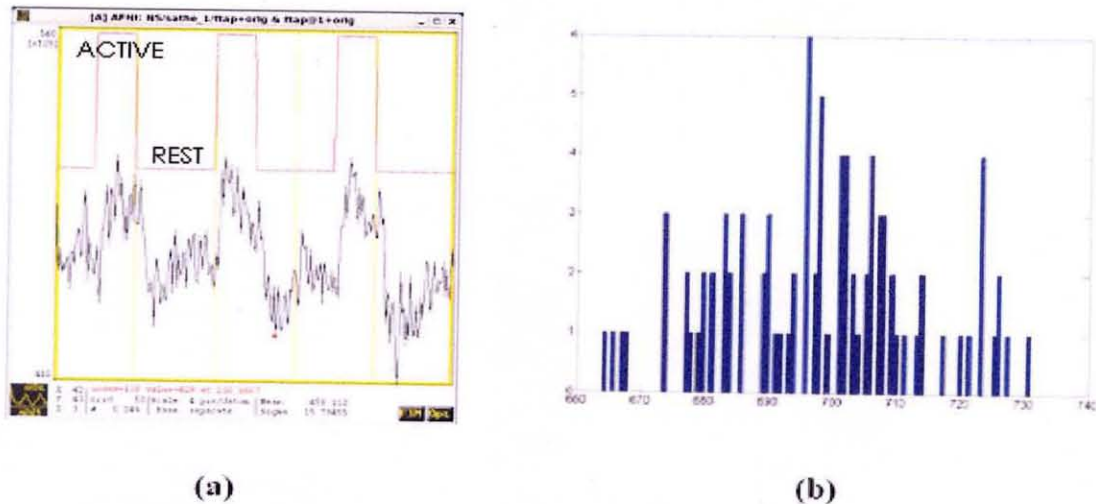
Figure 6.1 (a) Time series of finger tapping data and (b) histogram plotted for this time series.

To verify that these two states are distinct, the histogram was plotted for the entire time-series for an active voxel. It helped to check whether two different types of images were really discrete from each other. The threshold intensity values were determined from this histogram and were used to differentiate between two types ('Rest' and

'Active') of images. The intensity threshold values were used to generate activation maps. These maps showed that threshold values discerned some voxels very effectively between two states and thus it was concluded that these two images were separable.

6.1.2 Feature Selection

For feature selection of significant voxels from finger tapping data, correlation and ANOVA were used. Correlation technique was used to find the consistency of the fMRI response with the task. For this study, voxels having correlation values greater than 0.60 were considered active.

ANOVA was used to find the voxels which showed significant difference across two different conditions. The voxels having output probability values less than 0.1 were selected.
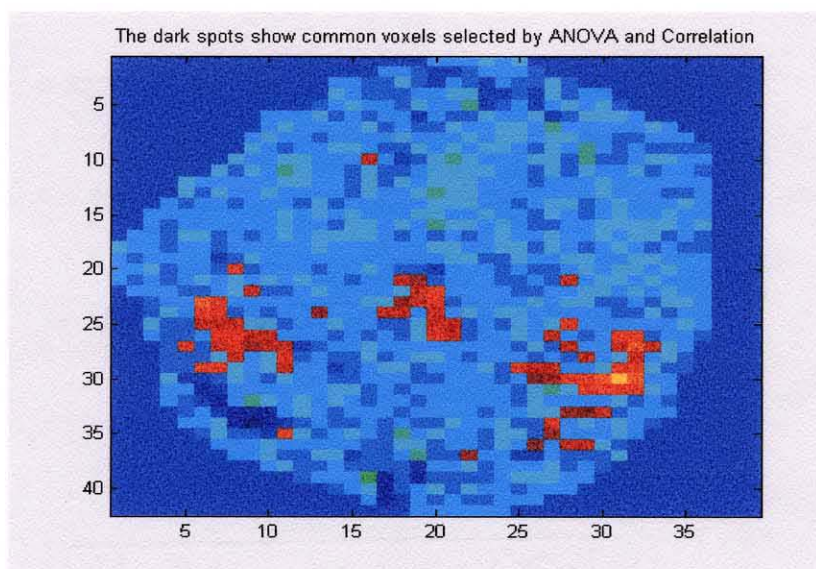
Figure 6.2 Feature selection performed on masked image of finger tapping data. Voxels in red color were selected jointly using ANOVA and correlation.

The common voxels found by both techniques were used as a pattern for classification task. Usually for finger tapping task, left and right sensory motor cortex regions show higher activities compared to other areas of brain and the voxels in the same area were found using feature selection (Figure 6.2).

Using criteria to select voxels that were active during both correlation and ANOVA helped decrease the number of voxels (dimensions) of the images which made the classification process faster. The number of selected voxels varied for different subjects which are shown in Table 6.1.

Table 6.1 Outcomes of Feature Selection Performed on Finger Tapping Data

	Total Voxels of the Image	Correlation CC > 0.6	ANOVA P < 0.05	Number of Voxels Commonly Selected by ANOVA and Correlation
Subject 1	1139	78	159	76
Subject 2	1377	50	270	50
Subject 3	1268	59	510	57
Subject 4	1379	98	322	97

6.1.3 Pattern Recognition

For binary classification, two different algorithms i.e., learning vector quantization (LVQ) and least square support vector machines (LS-SVM) were used. For classification using LVQ network, the learning rate was set to a default value of 0.1. Two hidden neurons were used because it was a binary classification and two layers were enough for this simpler classification. Ten epochs (learning steps to reach the target

output) were used for training, which were enough for network to reach the desired goal. As per the design of LVQ, number of inputs for both classes should be same.

In this study, 50 "Rest" and 50 "Active" patterns of selected voxels were used for training and a mixed group of 80 patterns was used for testing. The test images were not used for training or feature selection. Total compilation time for this algorithm (including feature selection, training and testing of data) was less than 15 seconds.

LS-SVM was also used for the same task but it accepts various numbers of inputs for different classes. For training, 50 "Active" and 80 "Rest" patterns were used and mixture of 80 patterns was used to test the trained model. For classification using LS-SVM, 'RFB' was selected as kernel type and model type was kept as 'CLASSIFIER'. The value of regularization parameters were found according to the size of the pattern. The γ and σ values were 80 and 75 respectively. The total compilation time for LS-SVM depends on the data size and the value of σ and for this experiment it was less than 20 seconds.

Both classification techniques gave similar and satisfactory outputs. For all four subjects, both classes ('Rest' and 'Active') were identified correctly. The rare cases of misclassification occurred for the images to be happened at the transition of the MR signal from one state to another. Approximately 10 % of test images in each subject were acquired during transition time. Hence, overall classification accuracy remained between 90% and 100%.

6.2 Results of Gas Mixture Data

6.2.1   Histogram Study

The histogram study was performed on multi-categorical gas mixture data to determine whether images were distinct enough for classification. The time-series of all five gas mixtures were concatenated and plotted as shown in Figure 6.3. From the time series, it was found that 2 % CO_2 and 5% CO_2 had the similar temporal patterns during rest and during breath hold. It was also observed that pattern for Carbogen had no significant difference between the rest and breath hold tasks. The temporal pattern for Oxygen was reversed compared to other gases as it had higher level of response for breath hold and lower level for normal breathing. The response pattern for air was similar to 2 % CO_2 and 5% CO_2 but the signal level was different than these two conditions.
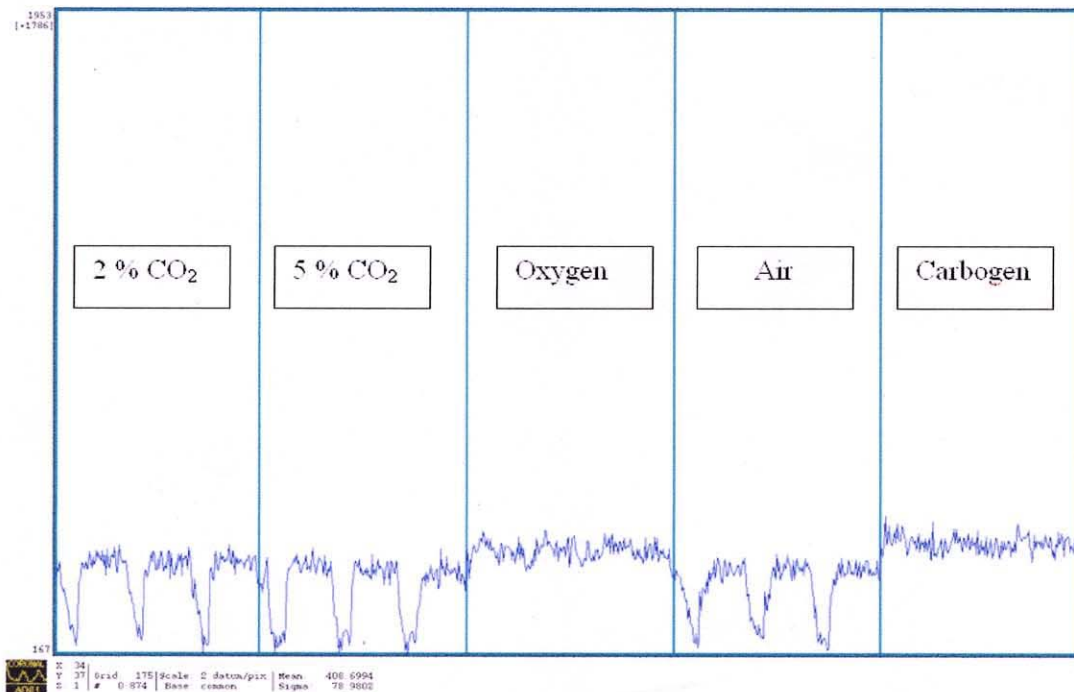
Figure 6.3 Time-series of fMRI responses for five different gas mixtures.

After the primary analysis of temporal responses for all conditions, the histogram was plotted for all ten categories (5 gas mixtures during rest and during breath hold) together to find out ten separate conditions. If each of the classes were distinct, it should show at least ten distinct peaks corresponding to each of the ten classes. But from the plot in Figure 6.4, it can be observed that ten different peaks could not be identified. This suggested that some of the fMRI responses were so similar that their histograms were simply overlapped.
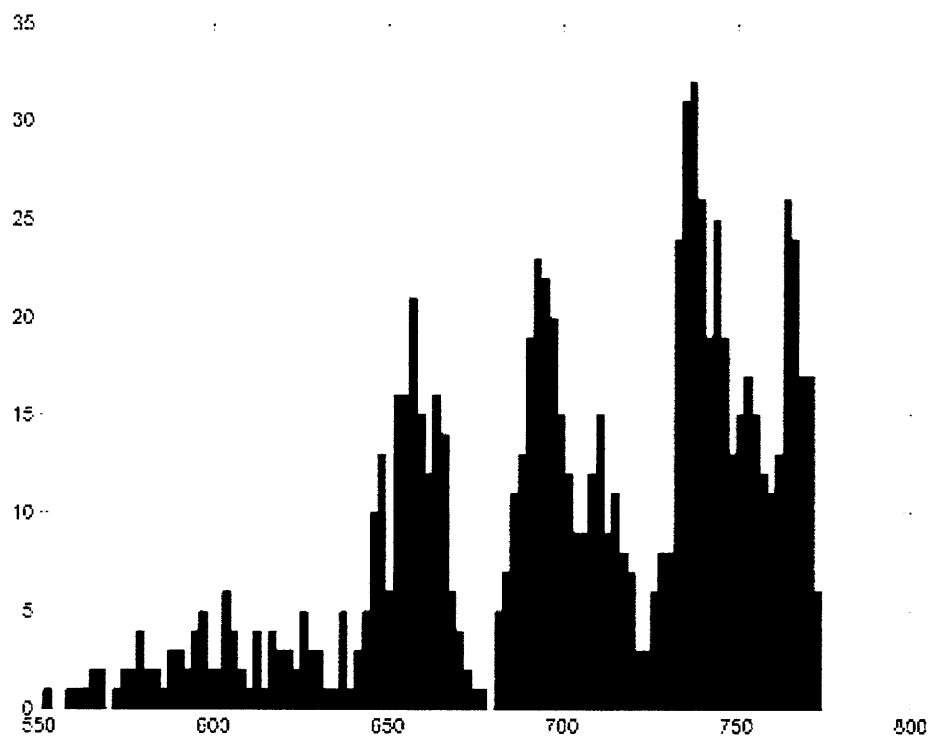
Figure 6.4 Histogram plot for five gas mixtures together.

The histogram helped to find out some threshold intensity values from the peaks. The images of all different conditions were plotted with highlighted voxels which had threshold intensities and they were compared. From theses images it was found that there

were distinctions in responses for normal breathing of 2 % CO_2, 5 % CO_2 and air but there was no such threshold value which can distinguish 2 % CO_2 from 5 % CO_2 at breath hold. It was also confirmed that Carbogen at breath hold had no difference from Carbogen at rest.

6.2.1 Feature Selection

The second experiment was the classification of images obtained from rats during different gas mixtures. Paired T-test was used for multi-categorical data was found not be very robust in detecting significant voxels in rat brain. A significance threshold of $p < 0.1$ was set for the initial selection of voxels. With the paired t-test, signal detection was performed between every possible pair of conditions, and to detect the significance voxels, only voxels that were detected in every pair of conditions were chosen. Using this method, very few voxels passed the significance level in all the possible combinations. The threshold value was not further reduced, because at lower threshold, the detected voxels were not significant, and could have occurred due to chance. As a consequence, t-test was not used for this method.

AVOVA which is typically faster was used as an alternative to the paired T-test. Further, the detection of significant voxels was more robust compared to the t-test. As a result, it was used for gas mixture data. Five images from each group were taken to perform ANOVA. The threshold value was set to select out the voxels of desired number for pattern recognition. Table 6.2 shows the threshold value and thus the number of voxels selected for each animal.

Table 6.2 Outcomes of Feature Selection Performed on Gas Mixture Data

	Total Voxels of the Image	Threshold for ANOVA	Number of Voxels Selected by ANOVA
Rat #1	334	$P < 0.0001$	222
Rat #2	384	$P < 0.00001$	220
Rat #3	409	$P < 0.0001$	189
Rat #4	364	$P < 0.0001$	179

6.2.2 Pattern Recognition

For classification of gas mixture images, LS-SVM was utilized. For normal breathing task, 75 patterns for each gas mixture and for breath holding task, 20 images for each gas mixture were used for training. Ten images from each category were selected for testing the classification algorithm. These test images were selected randomly and were not used for either training or feature selection. 'RBF' was selected as kernel type for this experiment also. The type of LS-SVM model was chosen as 'Function estimation' for multi-class classification task. The algorithm was previously tested to find most appropriate values of regularization parameters. The values of these parameters varied according to the size of the patterns. The classes for these images were determined according to their output values of function estimation. Ten different conditions as shown in Table 5.1 were attempted for pattern recognition.

The classification outcomes were not satisfactory for these ten categories. Therefore, it was decided to exclude those classes which were not enough distinct to be classified. From the histogram study, it was concluded that 2 % CO_2 was not very distinct from 5 % CO_2 breath hold and there was no distinction of Carbogen at rest from Carbogen at breath hold. Hence, two categories 2 % CO_2 at breath hold and Carbogen at

breath hold were excluded and pattern recognition was performed on remaining eight conditions.

The LS-SVM model was trained again for these eight patterns and tested for ten different sets of test patterns. Below are the tables showing classification outputs of ten test sets for all four animals. Each table has values of regularization parameters which were chosen for that particular dataset. The 'Y' shows the correct classification while 'X' is marked for false identification of the pattern. The accuracy of the each test run was calculated and shown in the last raw of each table. The average accuracy for all gas mixture data was 75%.

Table 6.3 Classification Results for Rat #1

Regularization parameters: $\gamma = 80$, $\sigma = 200$										
Test Set	1	2	3	4	5	6	7	8	9	10
2% CO_2 at REST	Y	Y	Y	Y	Y	Y	Y	Y	Y	Y
5% CO_2 at REST	Y	Y	Y	Y	Y	Y	Y	Y	Y	Y
OXYGEN at REST	Y	X	X	Y	Y	Y	X	Y	Y	X
AIR at REST	Y	Y	Y	Y	Y	Y	Y	Y	Y	Y
CARBOGEN at REST	Y	Y	Y	X	Y	X	Y	Y	Y	Y
5% CO_2 at BH	Y	Y	Y	Y	Y	Y	Y	X	Y	Y
OXYGEN at BH	Y	Y	X	X	X	Y	Y	Y	Y	X
AIR at BH	X	X	Y	Y	Y	Y	Y	X	Y	X
ACCURACY IN %	87.5	75	75	75	87.5	87.5	87.5	75	100	62.5

In the first animal the pattern was made up of 222 selected voxels and the σ was to set to 200 according to size of the pattern. From the above table it can be seen that 2% CO_2 at rest, 5% CO_2 at rest and air at rest were always classified correctly. The overall classification accuracy remained between 62.5% and 100% (Table 6.3).

Table 6.4 Classification Results for Rat #2

Regularization parameters: $\gamma = 80$, $\sigma = 200$										
Test Set	**1**	**2**	**3**	**4**	**5**	**6**	**7**	**8**	**9**	**10**
2% CO_2 at REST	Y	X	Y	Y	Y	Y	Y	Y	Y	Y
5% CO_2 at REST	Y	Y	X	Y	Y	Y	Y	Y	Y	Y
OXYGEN at REST	X	X	Y	X	Y	X	Y	Y	X	X
AIR at REST	Y	Y	Y	Y	Y	Y	Y	Y	Y	Y
CARBOGEN at REST	X	Y	Y	X	Y	X	Y	X	Y	Y
5% CO_2 at BH	Y	Y	Y	Y	Y	Y	Y	Y	Y	Y
OXYGEN at BH	X	X	Y	X	Y	X	X	X	X	X
AIR at BH	Y	Y	Y	Y	Y	Y	Y	Y	Y	Y
ACCURACY IN %	62.5	62.5	87.5	62.5	100	62.5	87.5	75	75	75

For the second animal, 220 voxels were selected by feature selection and σ was to set to 200. The classification results for this animal suggest that conditions of 2% CO_2 at rest, 5% CO_2 at breath hold and air at rest were classified 100% while, Carbogen at rest and Oxygen at rest were misclassified in many cases. For this animal also the overall accuracy remained between 62.5% and 100% (Table 6.4).

Table 6.5 Classification Results for Rat #3

Regularization parameters: $\gamma = 80$, $\sigma = 150$										
Test Set	**1**	**2**	**3**	**4**	**5**	**6**	**7**	**8**	**9**	**10**
2% CO_2 at REST	Y	Y	Y	Y	Y	Y	X	X	Y	Y
5% CO_2 at REST	Y	Y	X	Y	Y	Y	Y	Y	Y	Y
OXYGEN at REST	Y	Y	Y	Y	Y	Y	Y	Y	X	Y
AIR at REST	Y	Y	Y	Y	Y	Y	Y	Y	Y	Y
CARBOGEN at REST	Y	X	Y	Y	Y	Y	Y	Y	Y	Y
5% CO_2 at BH	X	X	Y	X	Y	Y	Y	X	Y	X
OXYGEN at BH	X	X	X	X	X	X	X	X	X	X
AIR at BH	X	X	Y	Y	X	X	X	X	Y	X
ACCURACY IN %	62.5	50	75	75	75	75	62.5	50	75	62.5

For third animal, the cases of misclassifications were more especially in patterns with breath hold task. Oxygen at breath hold was always classified incorrectly. From Table 6.2, it can be seen that only 189 voxels were selected from 409 when probability threshold was set to 0.0001. If these values are compared with values of first animal, it can be deduced that the images for this animal were less distinct for different conditions. And this could be the possible reason that the accuracy of pattern recognition for this animal was from 50% to 75% (Table 6.5).

Table 6.6 Classification Results for Rat #4

Regularization parameters: $\gamma = 80$, $\sigma = 150$										
Test Set	**1**	**2**	**3**	**4**	**5**	**6**	**7**	**8**	**9**	**10**
2% CO_2 at REST	Y	Y	Y	Y	Y	X	Y	Y	X	Y
5% CO_2 at REST	Y	Y	Y	Y	X	Y	X	Y	Y	Y
OXYGEN at REST	Y	Y	Y	Y	Y	X	Y	Y	X	Y
AIR at REST	X	Y	Y	X	Y	Y	X	Y	Y	X
CARBOGEN at REST	Y	Y	Y	Y	Y	Y	Y	Y	X	X
5% CO_2 at BH	X	X	X	X	X	X	X	X	X	X
OXYGEN at BH	Y	Y	X	Y	Y	X	X	X	X	X
AIR at BH	Y	Y		X	Y	Y	X	Y	Y	Y
ACCURACY IN %	75	87.5	75	62.5	75	50	50	75	37.5	50

In the fourth animal also, the misclassification occurred more in patterns of breath hold. The same reason as given for third animal can be counted for lower accuracies (Table 6.6).

The probability of getting 100% classification just by chance is 50% for binary classification and 12.5% for multi-class (eight classes) classification. In both present experiments, the outputs of classification were satisfactory and accuracies were well above chance.

CHAPTER 7

DISCUSSION AND CONCLUSION

7.1 Discussion

Pattern recognition finds the distinction between different datasets and develops a model that can identify the category of the unknown pattern. It is a useful technique for classification of fMRI images because for the given stimuli, small changes take place in only certain regions of the brain images. This method is helpful to distinguish among data sets that been obtained using different stimulus. In this study, both binary classification and multiclass classification was performed on fMRI data sets.

For the first experiment, when subjects tapped their fingers, the fMRI response was significantly higher than the baseline condition while, during rest the response was at baseline condition. Therefore, finger tapping data had unique "ON-OFF" pattern of fMRI response for two different conditions.

The second set of experiments involving ventilation of different gas mixtures had different BOLD responses from the brain. For 2% CO_2 and 5% CO_2 the temporal response patterns were similar. For 2% CO2, 5% CO2 and air, the MR signal remained high during breathing and got suppressed during breath hold in most cases. During Oxygen inhalation, the signal remained low at rest and it increased during breath hold. There was no signal change for Carbogen between rest and breath hold but the signal intensity for this gas mixture was higher than all other gases.

54

Classification accuracy depends on various factors and number of classes to be classified for each one of them. Binary classification is a relatively simpler task for fMRI images. But classification becomes more complex as the number of classes increase especially for fMRI data which are much overlapped. In second experiment, the low accuracy of classification can be because of various reasons. From the results of third and fourth animal (Table 6.5 and 6.6), it can be observed that cases of misclassifications are more for breath hold data than normal breathing. This might be due to fewer images of breath hold were available for training. Breath hold duration was 30 seconds and the task was repeated three times for each animal. After each 30 seconds, the animals were needed to be ventilated again to keep them alive. For each animal, breath hold task gave approximately 30 images. Out of these 30 images 20 were used for training which were not sufficient to train the model.

The second reason could be the classification algorithm itself. As mentioned before, the accuracy of LS-SVM model depends mostly on regularization parameters of the model. These values were found by grid search method which is the most convenient but an approximation method.

It is also possible that some images were not classified correctly because they were physiologically not significantly different. The time-series for 2% CO_2 and 5% CO_2 looked similar during rest as well during breath hold. It may be because there was no change occurring between MR signals for these two gases. It is possible that in the animal models being used for this study, 2% CO_2 was enough to saturate the signal and as a consequence there was no significant increase in 5% CO_2 when compared with 2% CO_2.

From this study, it can also be deduced that if for two different stimuli, the images are same and can not be classified, then there are chances that two stimuli different stimuli elicit similar physiological response in the brain.

Feature Selection techniques were proved useful to select effective number of voxels for efficient pattern recognition. The pattern recognition algorithm was performed with and without using feature selection. The classification was not significant without feature selection of effective voxels while, the classification accuracies were satisfactory when patterns made up of selected voxels were used. The correlation technique which was used for finger tapping data is helpful when the ideal response of particular stimulus is known. In this experiment, correlation compared the finger tapping data to the ideal "ON-OFF" pattern of the stimulus and found the effective voxels. Paired t-test which was used for multi-categorical data was a tedious task as it had to be performed individually on each possible pair of gas mixture conditions. ANOVA was the most convenient method for both experiments. It can be performed on multi-group data and desired number of voxels can easily be obtained by setting the threshold probability value.

There are few limitations of this study. The pattern recognition can be difficult task across the subjects. The pattern recognition algorithm compares the fMRI images voxels by voxel and thus it needs matching of the spatial patterns of the brain activity. The spatial matching across the subjects or animal models is difficult. There are few methods like ROI mapping and Talairach coordinates to register images across subjects but they harm the image resolution and thus the classification. The other limitation of pattern recognition is that the correct classification of unknown image is possible only if it belongs to one of the categories for which the classifier is trained.

Researchers are also trying to perform real time pattern recognition on fMRI data. Real time classification of fMRI images can be possible using fixed-block designs [21]. For real-time classification, the weights of the network can be updated with each new learning for better classification. For real-time classification of fMRI images, the required classifier should take very little time for training and get well along with the speed of the stimulus blocks. The real-time pattern recognition can be utilized in lie detection, brain-computer interfacing, etcetera.

7.2 Conclusion

The objective of this study was to perform pattern recognition to identify different physiological conditions of brain from fMRI images. The study was divided in two different experiments. The finger tapping data and gas mixture data were used for binary and multi-class classification, respectively. Motion correction helped removing motion artifacts and registering all images to the reference image. The mask was created to remove background voxels. Feature extraction helped to select effective voxels from fMRI images which actively responded to the given stimuli.

For finger tapping data, the two states 'Rest' and 'Active' were found to be very distinct by histogram study. They were classified correctly most of the times. The patterns used for classification were produced using voxels those were chosen by ANOVA and correlation techniques. These active voxels were found in right and left sensory motor cortex area which are most likely to be active during finger tapping task. Both classification tools, LVQ and LS-SVM were proved successful methods and gave classification accuracies more than 90%.

In the second experiment of gas mixture data, ten different conditions were to be classified. To find the significant voxels for classification, ANOVA was found to be the most robust method. From histogram study it was found that all ten conditions were not distinct and hence two conditions $2\%CO_2$ at breath hold and Carbogen at breath hold were eliminated. The classification algorithm was performed on remaining eight patterns. LS-SVM was used for classification of multi-categorical patterns and proved a successful classification devise. The classification accuracies were found between 37.5% and 100%, with an average accuracy of 70%.

From these two experiments, it can be said that pattern recognition is a useful tool to prepare the model which can classify the distinct physiological conditions of the brain. Feature selections methods are also very useful to extract the useful information from the overlapped fMRI images. The pattern recognition algorithm in conjunction with feature extraction can provide useful ways to analyze fMRI images.

REFERENCES

1. Norman KA, Polyn SM, Detre GJ, Haxby JV. Beyond mind-reading: multi-voxel pattern analysis of fMRI data. *Trends in Cognitive Sciences*. 2006;10: 424-430.

2. Cox DD & Savoy RL. Functional magnetic resonance imaging (fMRI) "brain reading": detecting and classifying distributed patterns of fMRI activity in human visual cortex. *Neuroimage*. 2003;19:261-270.

3. Kamitani Y & Tong F. Decoding the visual and subjective contents of the human brain. *Nature Neuroscience*. 2005;8:679-685.

4. Wang X, Hutchinson R & Mitchell T. Training fMRI classifiers to discriminate cognitive states across multiple subjects. *Advances in Neural Information Processing Systems* 2004,16:709-716.

5. Devlin H. Introduction to FMRI. FMRIB, Oxford. 2007. Available at: http://www.fmrib.ox.ac.uk/book/resources/education/fmri/. Accessed November 9, 2007.

6. Hornak JP. The Basics of NMR. 2006. Available at: http://www.cis.rit.edu/htbooks/nmr. Accessed November 4, 2007.

7. Bushberg JT & Seibert JA. *The Essential Physics of Medical Imaging*. 2nd ed. Philadelphia: Lippincott Williams & Wilkings; 2002.

8. Physics, Techniques and Procedures. Medcyclopedia. 2007. Available at: http://www.medcyclopaedia.com/library/topics/volume_i/t/t1_relaxation.aspx. Accessed October 8, 2007.

9. Hornak JP. FT imaging principles. Magnetic Resonance Imaging. 2000. Available at: http://astro.rit.edu/class/schp730/lect/lect-13.htm. Accessed November 4, 2007.

10. Huettel SA & Song AW. *Functional Magnetic Resonance Imaging*. Massachusetts: Sinauer Associates, Inc; 2004.

11. Cox RW. MCW AFNI – User manual. Milwaukee: Medical College of Wisconsin; 1996.

12. D'Agostino RB, Sullivan LM & Beiser AS. *Introductory Applied Biostatistics*. Ontario: Brooks/Cole, A Division of Thomson Learning, Inc; 2004.

13. Hill T & Lewicki P. *Statistics: Methods and Applications*. 1st ed., Oklahoma: StatSoft Inc; 2006.

14. Description. The Journal of the Pattern Recognition Society. 2007. Available at: http://www.elsevier.com/wps/find/journaldescription.cws_home/328/description# description. Accessed November 21, 2007.

15. Haykin S. *Neural Networks: A Comprehensive Foundation*. 2nd ed., New York: Macmillan Publishing; 1999.

16. Neural network toolbox. The MathWorks, Inc. 2007. Available at: http://www.mathworks.com/access/helpdesk/help/toolbox/nnet/. Accessed November 11, 2007.

17. LVQ neural nets. Portal on Forecasting with Artificial Neural Nertworks. 2005. Available at: http://www.neural-forecasting.com/lvq_neural_nets.htm. Accessed May 20, 2007.

18. Taylor JS & Cristianini N. *Support Vector Machines and other kernel-based learning methods*. Cambridge University Press; 2000.

19. Pelckmans K, Suykens J & Gestel T et al. LS-SVMlab toolbox user's guide version 1.5. *ESAT-SCD-SISTA Technical Report 02-145*. 2003. Available at: http://www.esat.kuleuven.ac.be/sista/lssvmlab. Accessed May 11, 2007.

20. Hsu C, Chang C & Lin C. A practical guide to support vector classification. 2007. Available at: http://www.csie.ntu.edu.tw/~cjlin/papers/guide/guide.pdf. Accessed May 15, 2007.

21. Yoo SS, FairnenyY & Chen NK et al. Brain-computer interface using fMRI: spatial navigation by thoughts. *NeuroReport*. 2004;15:1591-1595.